Synthesis and Photoisomerization of Fullerene– and Oligo(phenylene ethynylene)–Azobenzene Derivatives

Yasuhiro Shirai,[†,‡] Takashi Sasaki,[†] Jason M. Guerrero,[†] Byung-Chan Yu,[§] Phillip Hodge,[†] and James M. Tour[†,*]

[†]Department of Chemistry, Smalley Institute for Nanoscale Science and Technology, Rice University, MS-222, 6100 Main Street, Houston, Texas 77005, [‡]ICYS, National Institute for Materials Science, 1-1 Namiki, Tsukuba, Ibaraki 305-0044, Japan, and [§]Department of Chemistry, Mokwon University, Daejon 302-729, Republic of Korea

ABSTRACT The presence of fullerenes and oligo(phenylene ethynylene)s (OPEs) in azobenzene derivatives have a large effect on the photoisomerization behavior of the molecules. Fullerenes reduce the photoisomerization yield for *cis* isomers, and the OPEs, when directly attached to the azobenzenes, have a similar yet smaller effect when compared with the fullerenes. While these effects have not been previously considered for fullerene– and OPE–azobenzene derivatives, they were clearly detected in our work using NMR and UV–vis spectroscopy methods. The intramolecular electronic energy transfer between the fullerene and azobenzene moiety was examined in two cases in which separation of the two functional groups was small, as in 1, or large, as in 2. Almost no photoisomerization was observed for 1, while significant photoisomerization was observed for 2, apparently due to the effective isolation and blocking of electronic communication between the two functional groups.

KEYWORDS: fullerene · azobenzene · OPE · photoisomerization · molecular machines · nanomachines.

Advances in molecular science continue to facilitate the miniaturization of devices and the innovation of new molecule-based functional devices.[1–5] Of particular interest to our group is the design and synthesis of molecular machines that resemble macroscopic machinery; the ultimate goal of such work is the realization of useful nanomachines constructed using a "bottom-up" approach.[6,7] In the development of such molecular-sized devices and machines, the design scheme is quite different from that in the macroscopic world.[6–8] A strong understanding of both the functionality of molecular building blocks and the specific interactions between them is essential in the construction of devices and machines at the molecular scale.[9–11] Because the number of potential molecular building blocks continues to increase, we have focused on those that contain functionality such as electro- and photoactive components. The understanding of the interaction between these components has been gradually advanced.[12–14] In our previous study of the construction of a light-powered molecular vehicle, or a "motorized nanocar", we found that the motor unit was inoperative in the presence of fullerenes.[15] The result implied that rapid intramolecular energy transfer to the fullerene moiety quenched the photoexcited state of the motor moiety. Similar quenching of a photoexcited state with fullerenes has been reported.[16]

On the other hand, among the several photoisomerization processes studied previously, *cis–trans* photoisomerization of azobenzene chromophores has been extensively examined since their discovery in the late 1930s[17] and widely used, even to the present, in photoresponsive systems and devices.[18–21] The advantage of using azobenzenes is based on the large geometrical change accompanying *cis–trans* isomerization and their photostability, enabling the development of variety of photoresponsive functional devices such as smart polymers,[18] liquid crystals,[19] and molecular switches[20] and machines.[21] Recently, a hybrid of the azobenzene chromophore and fullerene was reported as a dendrimer having a fullerene in its core, and photoisomerization of the azobenzene moiety was briefly demonstrated.[22] The unique combination of the two functional groups, azobenzene chromophores and fullerenes, may lead to advances in the field of molecular switching because of the novel functional synergy.[23–25] However, no report on the properties of such hybrid materials has been published except for the brief communication on the dendritic fullerene derivatives.[22] In particular, the effect of the fullerene moiety on the photoisomerization behavior of the azobenzene has been overlooked. In the present work, it has been

*Adress correspondence to tour@rice.edu.

Received for review October 11, 2007 and accepted December 5, 2007.

Published online December 29, 2007.
10.1021/nn700294m CCC: $40.75

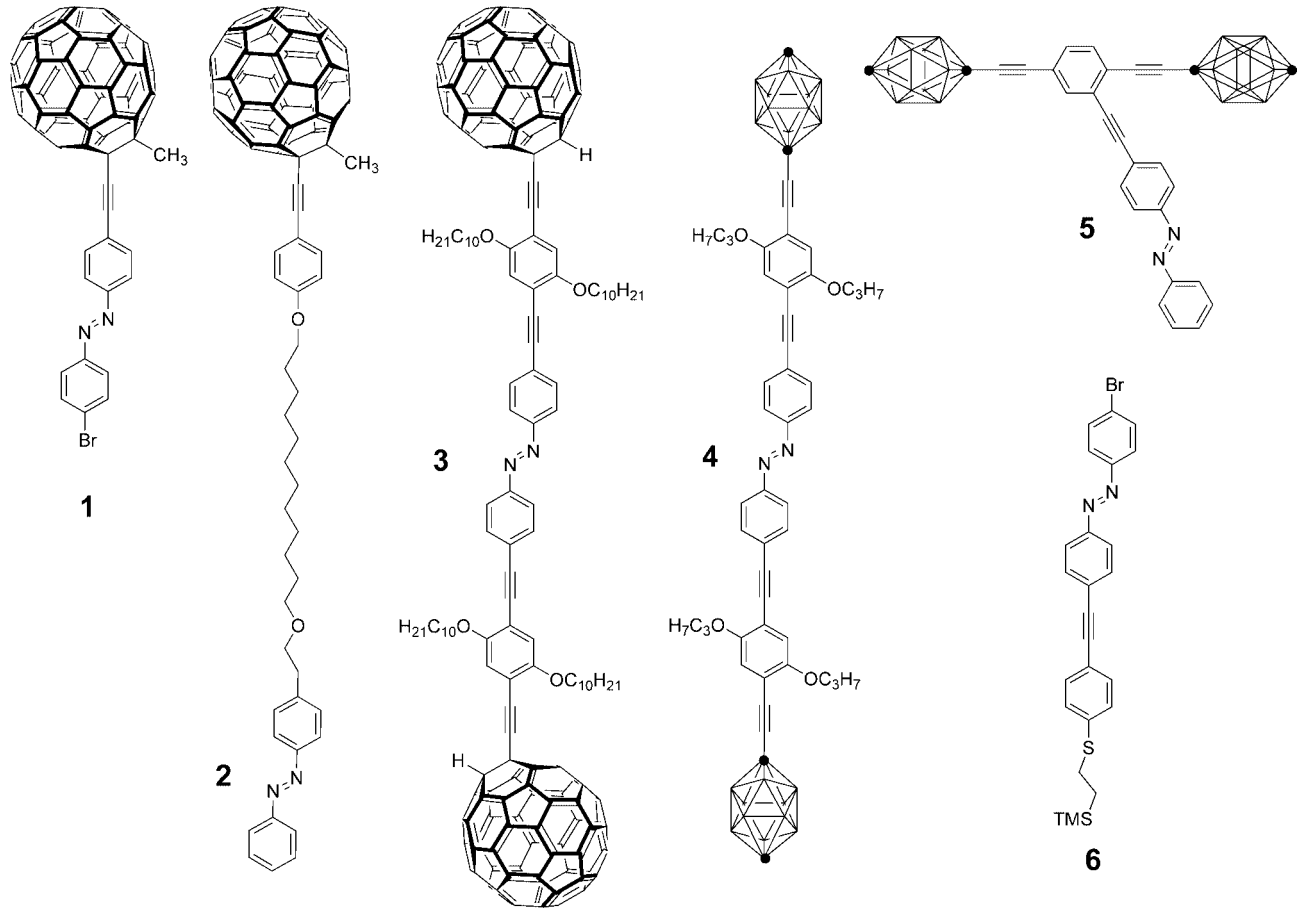

Figure 1. Fullerene−azobenzene hybrid and OPE-conjugated azobenzenes studied in this work. Compounds 4 and 5 contain *p*-carborane termini where the two darkened vertices are C and CH, *ipso* and *para*, respectively, and all other vertices are BH.

found that the presence of the fullerene can strongly affect the photoisomerization behavior of azobenzenes, and in some cases, quench photoexcitation of azobenzenes so that no photoisomerization occurs. This is in concert with findings in our previous work on the light-powered molecular motor[15] and that of others on stilbene−fullerene derivatives.[16]

It has also been found that oligo(phenylene ethynylene)s (OPEs) attached to an azobenzene moiety have a strong impact on its photoisomerization behavior. OPEs are an important class of organic building blocks for molecular device scientists because their shape-persistent nature and the relatively simple synthetic access facilitate the design and construction of devices with well-defined order.[26–30] Recently, the combination of the shape-persistent nature of OPEs and large geometrical changes of the azobenzene photoisomerization was used to generate dendrimers in which a large photomodulation of hydrodynamic volumes was achieved.[31]

Here we report the effect of fullerenes and OPEs on the photoisomerization behavior of azobenzene moieties using a variety of fullerene−azobenzene hybrid molecules and azobenzene derivatives (Figure 1) designed for UV–vis and NMR spectroscopic studies. The *cis*−*trans* photoisomerization of azobenzenes in the presence of fullerenes and OPEs only proceeds under certain conditions, and these conditions are delineated here.

RESULTS AND DISCUSSION

Energy transfer between the fullerene and azobenzene moieties occurs via intra- or intermolecular interactions, or a combination of both. We examined intermolecular interactions between pristine C_{60} and simple diiodo-azobenene[32] **14** using NMR spectroscopy. Intramolecular interactions between the functionalities were studied in two different cases, wherein the separation of the two functional groups was small, as in **1**, or large, as in **2**. The effect due to the presence of multiple fullerenes was examined with **3**. Finally, the effect due to the presence of OPEs was examined with structures **4**-**6** (Figure 1).

Design and Synthesis of Azobenzene Derivatives.

Fullerene−Azobenzene Hybrids. The details of the syntheses of fullerene−azobenzene hybrids **1**−**3** are given in Schemes 1–3. The structures were designed and synthesized to produce two extreme cases: where the fullerene and azobenzene moieties are close together as in structure **1** and where they are farther apart as in structure **2**. The difullerene derivative **3** was also synthesized to determine the effects of multiple fullerenes.

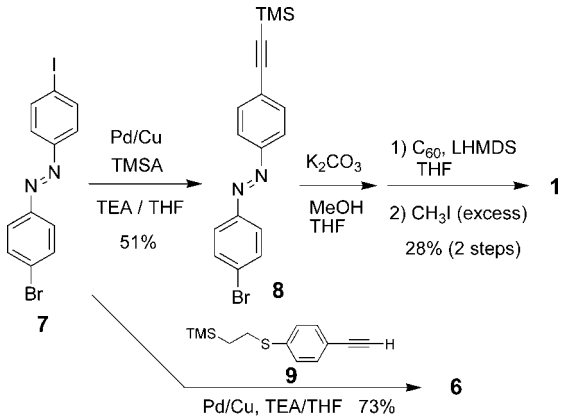

Scheme 1. Synthesis of the azobenzene derivatives 1 and 6. Pd/Cu = $PdCl_2(PPh_3)_2$, CuI.

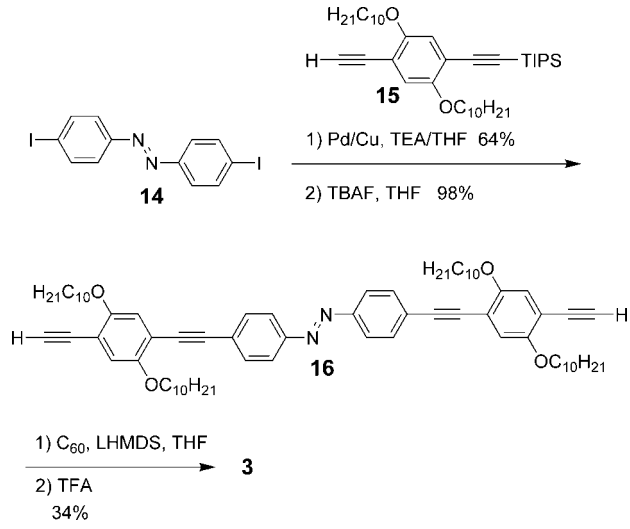

Scheme 3. Synthesis of the fullerene–azobenzene hybrid 3. Pd/Cu = $PdCl_2(PPh_3)_2$, CuI.

In Scheme 1, the azobenzene derivative **7**[33] was coupled with trimethylsilylacetylene (TMSA) to afford compound **8**, and then it was attached to the fullerene via the *in situ* ethynylation method[34] to afford **1**. For the isolation of the fullerene and the azobenzene moieties in **2**, we used a dodecyl alkyl chain for ease of synthesis and to produce a large isolation distance. Thus, in Scheme 2, **10**[33,35] was alkylated with dibromododecane using sodium hydride in DMF, and then the 4-iodophenol was alkylated to afford compound **12**. After the Pd-catalyzed coupling reaction with TMSA and the removal of the TMS group in tetra-*n*-butylammonium fluoride (TBAF), fullerene was attached using the *in situ* ethynylation method[34] to obtain the product **2** in 49% yield. In Scheme 3, the difullerene–azobenzene hybrid **3** was synthesized in a similar manner. The diiodoazobenzene (**14**) was coupled with compound **15**,[34,36] and following deprotection the fullerenes were attached via the *in situ* ethynylation method.[34]

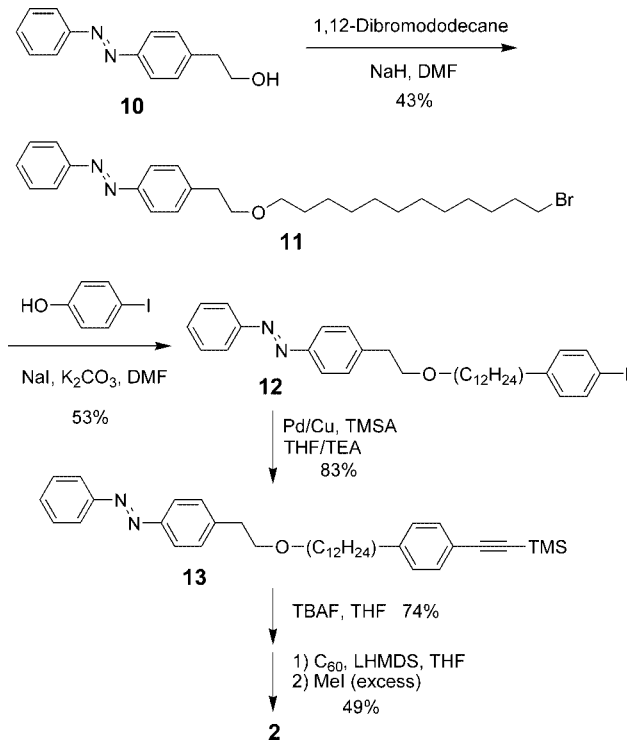

Scheme 2. Synthesis of the fullerene–azobenzene hybrid 2. Pd/Cu = $PdCl_2(PPh_3)_2$, CuI.

Azobenzene Derivatives with Conjugated OPEs. Addition of functional groups to the azobenzene moiety has various effects; it was thought that in addition to fullerenes, OPEs might also strongly affect their photoisomerization behavior. Because there are only a few reports on azobenzene–OPE conjugates[31–33] and there is no report on the photoisomerization yield of these azobenzene derivatives, it was decided to investigate this class of compounds. Schemes 4 and 5 outline the syntheses of the mono- (**5**) and di-OPE (**4**) substituted azobenzene derivatives. Another mono-OPE substituted azobenzene **6** was also prepared as an example of an OPE–azobenzene conjugate without carboranes (Scheme 1). The carboranes have no effect on the photoisomerization behavior of azobenzenes, and they were attached for other purposes in the later study of this class of compounds. It was found in previous work that the carborane will not interfere with the photoexcited state of a stilbene-like derivative, a molecular motor unit.[15] In Scheme 4, **19** was synthesized from 1,4-bis(propyloxy)-2,5-diiodobenzene (**17**)[37] by the Pd-catalyzed coupling reaction with TMSA followed by desilyl bromination.[38,39] The bromoalkyne **19** was then coupled with the *p*-carborane-copper adduct to afford the *p*-carborane-containing moiety **20**. The coupling reaction with **19** proceeded slowly, and 48 h was necessary for the reaction to be completed. This can be attributed to the electron-donating nature of the propyloxy groups present on the aryl ring that partially deactivate the alkynyl bromide toward oxidative

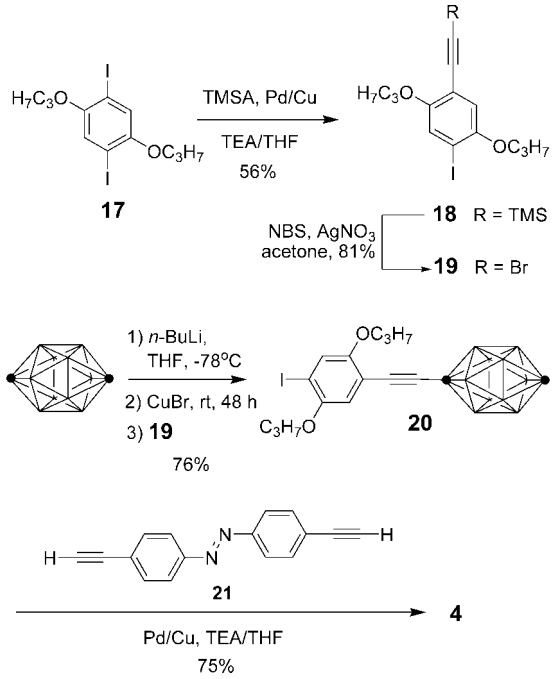

Scheme 4. Synthesis of the OPE–azobenzene hybrid 4. Pd/Cu = $PdCl_2(PPh_3)_2$, CuI.

addition by the organocopper reagent. Compound **20** was then coupled to **21**[40] to give the final product **4** in good yield. The mono-OPE substituted azobenzene **5** (Scheme 5) was synthesized in three steps from the iodo-azobenzene **22**.[33] Following the Pd-catalyzed coupling reaction with TMSA and the removal of the TMS group with TBAF, the dicarborane unit **25**[15] was coupled to afford the product **5**.

Intermolecular Energy Transfer between C_{60} and Azobenzenes. Intermolecular interactions between pristine C_{60} and the diiodoazobenene **14** were studied using NMR spectroscopy (Figure 2). The interaction was monitored using three different mixtures: 1:1 and 1:9 molar mixtures of C_{60} and **14** and **14** without C_{60}. Upon

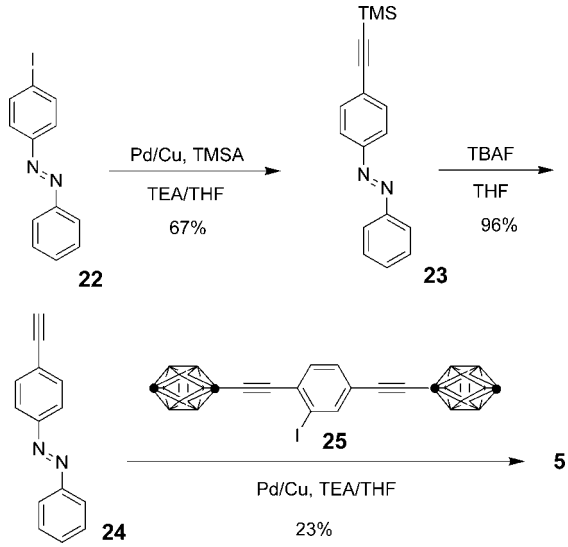

Scheme 5. Synthesis of the OPE–azobenzene hybrid 5. Pd/Cu = $PdCl_2(PPh_3)_2$, CuI.

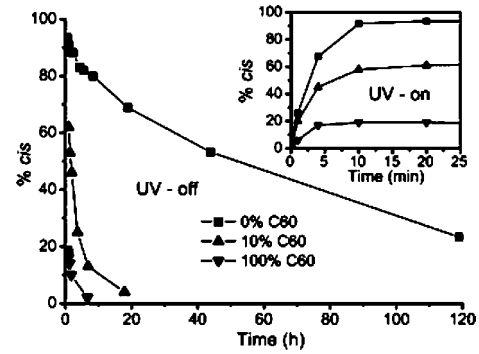

Figure 2. Changes in the amount of *cis* isomer of 14 in mixtures of 14 and C_{60} at three different molar ratios: 1:1 (100% C_{60}) and 9:1 (10% C_{60}) and no C_{60} (0% C_{60}) in the dark after establishing a photostationary state using 365 nm light. The inset shows *trans* to *cis* conversion in the same sample solutions during irradiation with light at 365 nm.

irradiation of these samples in a NMR tube with 365 nm light, the intensity of new peaks corresponding to the *cis* isomer of **14** increased with a concomitant decrease in the *trans* isomer peaks. Within 10 min of irradiation, a photostationary state (PSS) was achieved in all three cases (Figure 2, inset). Almost complete conversion from *trans* to *cis* isomer was achieved without C_{60}, while the conversion was decreased severely when even a small amount of C_{60} was present. The relaxation process from the *cis* to *trans* isomer in dark conditions at room temperature was also monitored following the same NMR peaks. It is clear from Figure 2 that C_{60} has a dramatic impact both on the photoisomerization yield and on the rate of the thermal relaxation process. The increase in the rate of conversion from the *cis* to *trans* isomer implies that the C_{60} catalyzes that isomerization. Catalytic activity of electron acceptors such as tetrachloroquinone on thermal isomerization of azobenzenes has been previously shown.[41] The decrease in the photoisomerization yield implies that the photoexcited singlet state of the azobenzene moiety is quenched by fullerenes via intermolecular electronic energy transfer. With the excitation at 365 nm, the pristine C_{60} should also be excited along with azobenzenes. In the diffusion-limited bimolecular process, however, only triplet–triplet energy transfer can take place because of the very short lifetime of the fullerene singlet excited state. The triplet excited energy level of the fullerenes (~35 kcal/mol)[42,43] is higher than that of the *cis* azobenzene derivatives (~29 kcal/mol) and comparable to that of the *trans* azobenzene derivatives (~35 kcal/mol).[44] Therefore, fullerenes could act as a triplet sensitizer rather than a quencher in the presence of the *cis* azobenzene derivatives. In fact, such bimolecular photoinduced energy transfer processes between pristine or functionalized fullerenes and many other compounds has been well studied.[42] It is also known that, in the triplet excited state, azobenzene derivatives favor *trans* isomers.[45–48] Therefore, as a quencher or a triplet sensitizer, fullerenes will always shift the isomer-

ization equilibrium of azobenzenes at the PSS to the *trans* isomers. Because the bimolecular reaction can be diffusion-limited, the intermolecular interactions should be suppressed under more dilute conditions. This was confirmed by the UV–vis spectroscopic study of the 1:1 molar mixture of **14** and C_{60} at 17 μM for both compounds, which is 100 times less concentrated than that of the NMR study. In this case, no decrease in the photoisomerization yield and no significant change in the rate of the thermal isomerization were observed over the time periods used in the former NMR study.

Intramolecular Energy Transfer in the Fullerene−Azobenzene Hybrid. Photoexcited properties of fullerenes including both pristine C_{60} and functionalized fullerenes are generally known for their low-lying excited electronic levels (~1.7 eV for singlet and ~1.5 eV for triplet).[42,43] These electronic levels are smaller than that of the lowest excited state S_1 of azobenzene derivatives (~2.9 eV).[44] An exothermic energy transfer from the excited azobenzene to the covalently linked fullerene in the fullerene−azobenzene hybrid can be expected. We investigated such intramolecular energy transfer processes using **1** and **2** (Figure 1). In **1**, the two functional moieties are isolated by one triple bond, and one sp^3-hybridized carbon atom isolates the fullerene π system from the azobenzene moiety. However, there is experimental evidence suggesting that there is a weak electronic interaction called periconjugation[49] between the fullerene and attached moieties; thus **1** can be treated as an example of a weakly conjugated fullerene−azobenzene hybrid. On the other hand, in **2**, the long saturated carbon chain between the azobenzene and the fullerene moieties should disrupt through-bond electronic communication between the two functional groups. These analyses can be experimentally supported by observing the electronic absorption spectra of the each functional moiety (Figures 3, and 4.) In **1**, the electronic transition (Figure 3, red line) is different from the sum of the original features of both functional groups (Figure 3, blue line), while the electronic transition of **2** (Figure 4, red line) remains unchanged from the sum of each component (Figure 4, blue line). These results suggest that there is no electronic communication in the isolated fullerene−azobenzene hybrid **2**, and there is a strong interaction in the conjugated fullerene−azobenzene hybrid, **1**.

Upon irradiation of each solution (17 μM) at 365 nm (Figure 3) or 334 nm (Figure 4), the azobenzene moiety underwent photoisomerization from *trans* to *cis* with a characteristic decrease in the 320–370 nm band. However, the change in the absorption (Δabs) of **1** was extremely small. This may indicate an efficient electronic energy transfer between the azobenzene and fullerene moieties, as predicted from its conjugated structure. From the Δabs of **1** (0.03) and **8** (0.33) in Figure 3, the photoisomerization yield of **1** is estimated to be about 10% of that of **8** (no fullerene moiety). On the other hand, from the Δabs of **2** (0.025) and **13** (0.07) in Figure 4, the photoisomerization yield for **2** was about 35% of **13** (no fullerene moiety). The 1:1 molar mixture of the pristine C_{60} and the compounds without a fullerene moiety (**8** and **13**) showed no decrease in the photoisomerization yield (blue lines in Figures 3 and 4), indicating that there is no significant intermolecular effect at the studied conditions. Although the length of separation between the two functional moieties in **2** is 3 nm when displayed as drawn in Figure 1, the actual distance is likely much closer in solution due to the flexibility of the alkyl chain. The decrease in the photoisomerization yield for **2** was much smaller than that of the conjugated azobenzene−fullerene hybrid **1**. The result clearly indicates that the isolation of the two func-

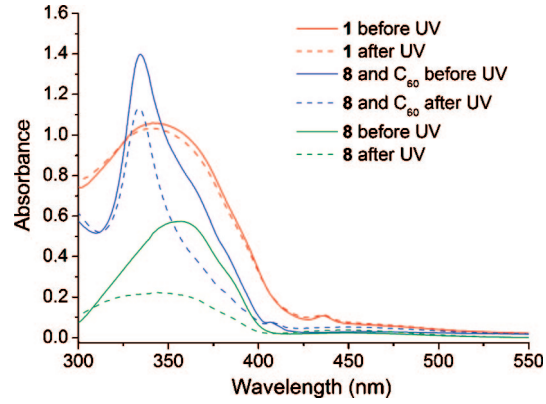

Figure 3. Absorption spectra of 1, 8, and 1:1 mixture of 8 and C_{60} (chloroform, ~17 μM). Upon irradiation with 365 nm light for 10 min, the electronic transitions at ~357 nm were decreased in all cases, and the PSS was achieved (change in absorbance at 357 nm was 0.05 (1), 0.33 (8), and 0.33 (mixture of 8 and C_{60})). Due to the electronic communication between the fullerene and azobenzene moieties, the absorption spectrum of 1 (red line) is significantly different from the sum of the spectrum for 8 and C_{60} (blue line).

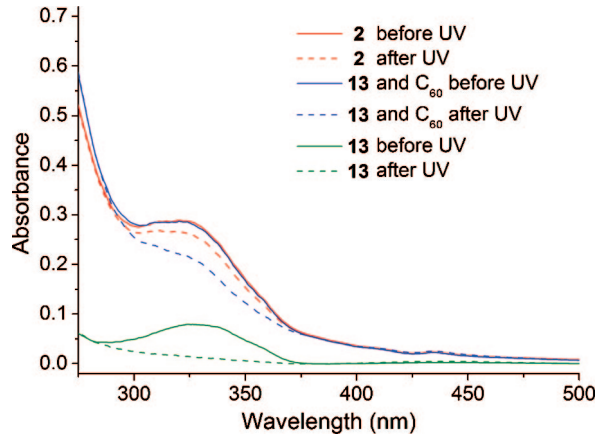

Figure 4. Absorption spectra of 2, 13, and 1:1 mixture of 13 and C_{60} (chloroform, ~4 μM). Upon the irradiation with 334 nm light for 5 min, the electronic transitions at ~330 nm were decreased in all cases, and the PSS was achieved (change in absorbance at 330 nm was 0.025 (2), 0.07 (13), and 0.07 (mixture of 13 and C_{60})). Absorption spectrum of 2 (red line) is almost identical to the sum of the spectrum for 13 and C_{60} (blue line), suggesting that there is no electronic communication between the two functional groups.

TABLE 1. Photoisomerization Yield at the PSS for Various Azobenzene Derivatives

type	compound	% *cis*	excitation wavelength (nm)
fullerene azobenzene mixtures	**14**	>90[a]	365
	14 + C_{60} (10%)	58[a]	365
	14 + C_{60} (100%)	19[a]	365
fullerene−azobenzene conjugated hybrid	**1**	<10[b]	365
	8	>90[a,b]	365
fullerene−azobenzene isolated hybrid	**2**	~35[b]	334
	13	>90[a,b]	334
difullerene−azobenzene hybrid	**3**	~0[a,b]	365
azobenzene−OPE hybrid	**4**	22[a]	436
	5	48[a]	365
	6	46[a]	365

[a]Photoisomerization yield was determined by NMR. [b]Photoisomerization yield was estimated by UV–vis.[50–52]

tional groups has some effect. Nevertheless, the physical separation of the π-systems has a marked effect on the isomerization of the azobenzene.

Effect of the Conjugated OPEs Attached to the Azobenzene Moiety. Finally, we examined the effect of OPEs on the photoisomerization behavior of azobenzene chromophores. Because of the shape-persistent nature of OPEs and their simplicity of design and synthesis, many molecular devices and machines use OPEs in the molecular framework.[26–30] However, not many examples of azobenzene derivatives incorporated into OPEs have been reported,[31–33] and there is no report on the effect of OPEs on the photoisomerization yield of azobenzene derivatives. The photoisomerization yield for each OPE−azobenzene derivative **4**−**6** was determined using NMR, and the results are summarized in Table 1. In this work, the following trend was observed: as the number of OPEs attached to the azobenzene moiety was increased, a significant decrease in the photoisomerization yield at the PSS was observed. Thus, when only one OPE was attached to the azobenzene (**5** and **6**), the photoisomerization yield was reduced to ~50% of that of the azobenzene derivative without any OPEs (**8**), while the yield was further reduced to less than 25% when two OPEs were attached as in **4**. The other noticeable feature of the disubstituted azobenzene **4** was the red shift of the azobenzene absorption band due to the elongated conjugation along the OPE backbone (see Figure S1-1 in the Supporting Information for the UV–vis spectrum of **4**). Visible light at ~436 nm was necessary to achieve the highest conversion to *cis* isomer in this case. As expected from the other fullerene−azobenzene hybrids, the difullerene and OPE-substituted derivative **3** showed no photoisomerization. Because **4**, which is similar to **3** but with carboranes instead of fullerenes, showed a small but noticeable photoisomerization yield, the data suggests that the severe deactivation of **3** is due, in large part, to the presence of the two fullerene moieties.

CONCLUSIONS

It has been shown that fullerenes and OPEs have a large effect on the photoisomerization behavior of azobenzene derivatives (Figure 1). Fullerenes can severely reduce the photoisomerization yield for *cis* isomers, while OPEs directly attached to the azobenzenes have a noticeable but smaller effect. These trends have not been previously considered for fullerene− and OPE−azobenzene derivatives but were clearly detected in this work using NMR and UV–vis spectroscopies. Fullerenes, OPEs, and azobenzenes are examples of common molecular device building blocks; however, when they are combined together to form more complex systems, the present work underscores that their synergistic effects must be considered.

MATERIALS AND METHODS

General Methods. All reactions were performed under an atmosphere of nitrogen unless stated otherwise. Precursors **7**,[33] **9**,[53] **10**,[33,35] **14**,[32] **15**,[34,36] **17**,[37] **18**–**20**,[54] **21**,[40] **22**,[33] and **25**[15] were prepared according to literature procedures. Reagent grade diethyl ether and THF were distilled from sodium benzophenone ketyl. Triethylamine (TEA) and CH_2Cl_2 were distilled over CaH_2. Fullerene (99.5+% pure) was purchased from MTR Ltd. and used as received. Lithium hexamethyldisilazide (LHMDS; 1 M solution in THF) and TBAF (1 M solution in THF) were obtained from Sigma-Aldrich and used as received. Flash column chromatography was performed using 230–400 mesh silica gel from EM Science. Thin layer chromatography was performed using glass plates precoated with silica gel 40 F_{254} purchased from EM Science. Melting points were uncorrected. The ultrasonicated fullerene slurry in THF was prepared in general ultrasonic cleaners.

NMR and UV–vis spectroscopy irradiation experiments were performed in deoxygenated solutions at ~1.7 mM (NMR) or 4−17 μM (UV–vis) using a 100 W Hg arc light source (EFOS Acticure A4000 UV light source/curing system) with appropriate wavelength Hg line filters (Andover) and band-pass filters. The light intensity after passing through the filters was monitored with a radiant power meter (Oriel). Typical light intensity for NMR experiments was 10−50 mW/cm^2 and up-to 10 mW/cm^2 for UV–vis experiments. The rate of the thermal isomerization for all experiments was slow enough to allow the determination of the photoisomerization yields at the PSS without significant change using normal NMR and UV–vis operations (measured within 1−3 min after reaching the PSS). In all experiments, reversibility of the photoisomerization process was checked by irradiating the sample solutions with appropriate wavelength cut-on long-pass filters or by keeping the samples in the dark to induce *cis*−*trans* reverse isomerization. *ChemDraw* 9.0 was used in naming the compounds.

General Procedure for the Coupling of a Terminal Alkyne with an Aryl Halide Using a Palladium-Catalyzed Cross-Coupling (Sonogashira) Protocol. To an oven-dried round-bottom flask equipped with a magnetic stir bar were added the aryl halide, the terminal alkyne, $PdCl_2(PPh_3)_2$ (ca. 2 mol % per aryl halide), and CuI (ca. 4 mol % per aryl halide). A solvent system of TEA, THF, or both was added depending on the substrates. Upon completion, the reaction was quenched with a saturated solution of NH_4Cl. The organic layer was then diluted with hexanes, diethyl ether, or CH_2Cl_2 and washed with water or saturated NH_4Cl (1×). The combined aqueous layers were extracted with hexanes, diethyl ether, or

CH_2Cl_2 (2×). The combined organic layers were dried over $MgSO_4$ and filtered, and the solvent was removed from the filtrate *in vacuo* to afford the crude product, which was purified by column chromatography (silica gel). Eluents and other slight modifications are described below for each compound.

General Procedure for the Addition of C_{60} to Terminal Alkynes Using LHMDS, *in Situ* Ethynylation Method. To an oven-dried round-bottom flask equipped with a magnetic stir bar were added the terminal alkyne and C_{60} (2 equiv per terminal alkyne H). After adding THF, the mixture was sonicated for at least 3 h. To the greenish-brown suspension formed after the sonication was added LHMDS dropwise at room temperature over 0.5−1.5 h. As the reaction progressed, the mixture turned into a deep greenish-black solution. During the addition of the LHMDS, small aliquots from the reaction were extracted and quenched with trifluoroacetic acid (TFA), dried, and redissolved in CS_2 for TLC analysis (developed in a mixture of CS_2, CH_2Cl_2, and hexanes). Completion of the reaction was confirmed by the disappearance of the starting materials. The reaction was usually complete within 1.5 h from the beginning of the LHMDS addition. Upon completion, the reaction was quenched with TFA or MeI to give a brownish slurry. When MeI was used, the reaction was stirred at room temperature for at least 6 h. Excess TFA or MeI and solvent were then removed *in vacuo* to afford a crude product that was purified by flash column chromatography (silica gel). Eluents and other slight modifications are described in the following experiments for each compound.

Compound 1. To a round-bottom flask equipped with a magnetic stirrer was added compound **8** (0.109 g, 0.305 mmol), THF/MeOH (1:1, 30 mL), and K_2CO_3 (0.15 g, 1.09 mmol). The reaction mixture was stirred at room temperature for 2 h, then quenched with water and diluted with hexanes. The aqueous layer was extracted with CH_2Cl_2 (×3). The combined organic layers were dried over $MgSO_4$, filtered, and concentrated under vacuum. The crude material was filtered through a plug of silica gel using CH_2Cl_2/hexanes mixture and subjected to the general *in situ* ethynylation procedure with C_{60} (0.184 g, 0.255 mmol), THF (25 mL), LHMDS (0.9 mL, 0.9 mmol), and MeI (6 mL). Crude products were dissolved in CS_2 and directly loaded onto flash column and eluted with 100% CS_2. The product was further purified using another flash column with graduate elution of 1–25% CS_2 in hexanes to afford the product **1** (73.5 mg, 28%) as a brown solid. FTIR (KBr) 2968, 1735, 1360, 1208, 834, 524 cm^{-1}; ^1H NMR (CS_2/$CDCl_3$ (2:1), 400 MHz) δ 8.04 (d, J = 8.7 Hz, 2H), 7.92 (d, J = 8.7 Hz, 2H), 7.87 (d, J = 8.7 Hz, 2H), 7.69 (d, J = 8.7 Hz, 2H), 3.59 (s, 3H); ^{13}C NMR (CS_2/$CDCl_3$ (2:1), 100 MHz) δ 156.8, 153.0, 151.9, 151.2, 147.9, 147.8, 146.6, 146.5, 146.4, 146.3, 145.9, 145.7, 145.6, 145.5, 145.4, 145.2, 145.0, 144.8, 144.7, 143.3, 142.71, 142.67, 142.24, 142.18, 142.17, 142.1, 141.7, 141.6, 140.4, 140.2, 134.6, 134.4 (30 signals from sp^2-C in the C_{60} core), 133.0, 132.4, 126.3, 125.6, 124.6, 123.4, 91.1, 85.2, 61.7 (*C*CH_3 in the C_{60} core), 59.8 (quaternary sp^3-C in the C_{60} core), 33.0; MALDI-TOF MS *m/z* (sulfur as the matrix) calcd for $C_{75}H_{11}BrN_2$ 1018, found 1019 (M^+).

Compound 2. To a round-bottom flask equipped with a magnetic stirrer was added compound **13** (0.155 g, 0.266 mmol), THF (10 mL), and TBAF (0.5 mL, 0.5 mmol). The reaction mixture was stirred at room temperature for 20 min, then quenched with water and diluted with CH_2Cl_2. The aqueous layer was extracted with CH_2Cl_2 (×3). Combined organic layers were dried over $MgSO_4$, filtered, and concentrated under vacuum. Crude material was purified by flash column with gradually increasing 1–35% CH_2Cl_2 in hexanes to afford deprotected product (0.1 g, 74%) as a yellow powder. ^1H NMR ($CDCl_3$, 400 MHz) δ 7.92 (d, J = 6.9 Hz, 2H), 7.86 (d, J = 8.5 Hz, 2H), 7.52–7.46 (m, 3H), 7.42 (d, J = 8.9 Hz, 2H), 7.38 (d, J = 8.5 Hz, 2H), 6.83 (d, J = 8.9 Hz, 2H), 3.95 (t, J = 6.6 Hz, 2H), 3.68 (t, J = 7.0 Hz, 2H), 3.45 (t, J = 6.6 Hz, 2H), 2.99 (s, 1H), 2.97 (t, J = 7.0 Hz, 2H), 1.86–1.83 (m, 2H), 1.55 (m, 2H), 1.40 (m, 2H), 1.31–1.27 (m, 14H); ^{13}C NMR ($CDCl_3$, 100 MHz) δ 159.8 (aryloxy sp^2-C in the aromatic ring), 153.0, 151.5, 143.0, 133.8, 131.00, 129.8, 129.3, 123.1, 123.0, 114.7, 114.1, 84.0, 75.8, 71.6, 71.4, 68.3, 36.5, 29.9, 29.81, 29.79, 29.77, 29.68, 29.59, 29.4, 26.4, 26.2. This product (0.1 g, 0.196 mmol) was subjected to the general *in situ* ethynylation procedure with C_{60} (0.18 g, 0.25 mmol), THF (150 mL), LHMDS (1.0 mL, 1.0 mmol), and MeI (3 mL). Crude products were dissolved in CS_2 and directly loaded onto a flash column and eluted with CS_2/CH_2Cl_2/hexanes at 100:1:1, then 5:2:3. The product was dissolved in a minimum amount of CS_2 and further purified using another flash column with graduate elution with CS_2/CH_2Cl_2/hexanes at 1:1:100, 5:2:3, and 4:3:3 to afford the product **2** (0.12 g, 49%) as a brown solid. FTIR (KBr) 2908, 2832, 1599, 1507, 1388, 1246, 823, 524 cm^{-1}; ^1H NMR ($CDCl_3$, 400 MHz) δ 7.92 (d, J = 7.0 Hz, 2H), 7.86 (d, J = 8.4 Hz, 2H), 7.72 (d, J = 8.8 Hz, 2H), 7.52–7.46 (m, 3H), 7.39 (d, J = 8.4 Hz, 2H), 6.98 (d, J = 8.8 Hz, 2H), 4.04 (t, J = 6.6 Hz, 2H), 3.69 (t, J = 7.1 Hz, 2H), 3.53 (s, 3H), 3.46 (t, J = 6.6 Hz, 2H), 2.98 (t, J = 7.1 Hz, 2H), 1.84 (m, 2H), 1.59 (m, 2H), 1.50 (m, 2H), 1.34–1.26 (m, 14H); ^{13}C NMR ($CDCl_3$, 100 MHz) δ 160.0 (aryloxy sp^2-C in the aromatic ring), 157.5, 154.1, 153.0, 151.5, 148.0 (×2), 146.8, 146.7, 146.6, 146.5, 146.3, 145.8 (×2), 145.7, 145.58, 145.57, 145.4, 145.04, 145.0, 143.4, 143.0, 142.88, 142.85, 142.45, 142.41, 142.39, 142.36, 141.9, 141.8, 140.5, 140.4, 134.701, 134.695, 133.8 (30 signals from sp^2-C in the C_{60} core), 131.0, 129.9, 129.3, 123.1, 123.0, 115.0, 114.6, 86.9, 85.6, 71.6, 71.4, 68.4, 62.0 (*C*CH_3 in the C_{60} core), 60.1 (quaternary sp^3-C in the C_{60} core), 36.5, 33.2, 29.9, 29.83, 29.82, 29.80, 29.7, 29.6, 29.4, 26.4, 26.3; MALDI TOF MS *m/z* calcd for $C_{95}H_{44}N_2O_2$ 1245, found 1245.

Compound 3. See the general procedures for the *in situ* ethynylation C_{60}. Materials used were **16** (0.06 g, 0.058 mmol), C_{60} (0.17 g, 0.23 mmol) in THF (100 mL), and 10 equiv of LHMDS (0.58 mL). After quenching with TFA, the resulting residue was purified by 5:3:2 CS_2/hexane/CH_2Cl_2 to afford **3** (0.049 g, 34%) as a dark brown solid. FTIR (KBr) 2914, 2849, 1595, 1497, 1377, 1274, 1209, 1019, 834, 525 cm^{-1}; ^1H NMR (400 MHz, $CDCl_3$:CS_2 (1:1)) δ 7.95 (d, J = 8.6 Hz, 4H), 7.66 (d, J = 8.6 Hz, 4H), 7.22 (s, 2H), 7.16 (s, 2H), 7.09 (s, 2H), 4.17 (t, J = 6.2 Hz, 4H), 4.13 (t, J = 6.4 Hz, 4H), 1.96 (m, 8H), 1.65 (m, 8H), 1.50–1.39 (m, 12H), 1.34–1.23 (m, 36H), 0.91 (t, J = 7.0 Hz, 6H), 0.87 (t, J = 7.0 Hz, 6H); ^{13}C NMR (125 MHz, $CDCl_3$:CS_2 (1:1)) δ 154.0, 153.5 (2 signals from aryloxy sp^2-C in the aromatic ring), 151.3, 151.2, 151.0, 147.4, 147.1, 146.4, 146.15 (×2), 145.99 (×2), 145.5, 145.42. 145.39, 145.3, 145.2, 145.1, 144.5, 144.3, 143.0, 142.39, 142.36, 141.83, 141.78, 141.70, 141.68, 141.5, 141.4, 140.2, 140.1, 135.9, 134.9 (30 signals from sp^2-C in the C_{60} core and one signal from sp^2-C in the aromatic ring), 132.1, 126.2, 123.0, 116.5, 116.3, 114.2, 113.1, 97.5, 95.2, 89.3, 80.5, 69.14, 69.06, 61.8 (*C*H in the C_{60} core), 55.2 (quaternary sp^2-C in the C_{60} core), 32.0, 29.78, 29.76, 29.64, 29.55, 26.6, 26.3, 23.0, 14.3; EI-MS *m/z* calcd for $C_{192}H_{98}N_2O_4$ 2494.75, found 2495.

Compound 4. See general procedure for the Pd/Cu coupling reaction. The materials used were **20** (0.005 g, 0.024 mmol), **21** (0.021 g, 0.043 mmol), $PdCl_2(PPh_3)_2$ (0.002 g, 0.003 mmol), CuI (0.001 g, 0.005 mmol), TEA (5 mL), and THF (10 mL) at room temperature overnight. The residue was purified by flash column chromatography with a gradual increase of 5–10% CH_2Cl_2 in hexanes to give product **4** (0.015 g, 75%) as an orange powder. FTIR (KBr) 2920, 2849, 2208, 2154, 1600, 1464, 1225, 851 cm^{-1}; ^1H NMR (400 MHz, $CDCl_3$) δ 7.90 (d, J = 8.8 Hz, 4H), 7.64 (d, J = 8.8 Hz 4H), 6.93 (s, 2H), 6.77 (s, 2H), 3.94 (t, J = 6.5 Hz, 4H), 3.89 (t, J = 6.3 Hz, 4H), 3.22–1.93 (broad m, 22H), 1.89–1.78 (m, 8H), 1.12–1.05 (m, 12H); ^{13}C NMR (125 MHz, $CDCl_3$) δ 154.3, 153.5, 151.8, 132.4, 126.3, 123.0, 116.9, 116.7, 114.4, 112.3, 94.8, 88.6, 76.0, 71.1, 70.9, 29.7, 22.7, 10.6; EI-HRMS *m/z* calcd for $C_{48}H_{62}B_{20}N_2O_4$ 950.66, found 950.7.

Compound 5. See the general procedure for the Pd/Cu coupling reaction. The materials used were **24** (0.054 g, 0.26 mmol), **25** (0.140 g, 0.26 mmol), $PdCl_2(PPh_3)_2$ (0.007 g, 0.0104 mmol), CuI (0.004 g, 0.0208 mmol), TEA (0.3 mL), and THF (3.7 mL) at room temperature overnight. The residue was purified by flash column chromatography with 10% CH_2Cl_2 in hexanes to give product **5** (0.037 g, 23%) as a red-orange oil. FTIR (KBr) 3066, 2919, 2849, 2610, 1605, 1497, 1057, 845, 758 cm^{-1}; ^1H NMR (500 MHz, $CDCl_3$) δ 7.98 (m, 4H), 7.71 (d, J = 9.0 Hz, 2H), 7.56–7.50 (m, 3H), 7.46 (dd, J = 1.5, 0.5 Hz, 1H), 7.25 (dd, J = 8.0, 0.5 Hz, 1H), 7.16 (dd, J = 8.0, 1.5 Hz, 1H), 3.0–1.9 (broad m, 22H); ^{13}C NMR (125 MHz, $CDCl_3$) δ 152.6, 152.1, 135.1, 132.6, 132.1, 131.3, 131.1, 129.1, 126.2, 125.2, 124.0, 122.97, 122.96, 122.0, 94.0, 91.2, 88.7, 87.9, 77.8, 77.6, 69.3, 69.0, 60.4 (×2); EI-HRMS *m/z* calcd for $C_{28}H_{34}B_{20}N_2$ 615.4713, found 615.4708.

(*E*)-1-(4-Bromophenyl)-2-(4-((4-(2(trimethylsilyl)ethylthio) phenyl)ethynyl)phenyl)diazene (6). See the general procedure for the Pd/Cu coupling reaction. The materials used were **7** (0.202 g, 0.565 mmol), **9** (0.188 g, 0.802 mmol), $PdCl_2(PPh_3)_2$ (0.012 g, 0.017 mmol), CuI (0.006 g, 0.031 mmol), TEA (10 mL), and THF (20 mL) at room temperature overnight. The residue was purified by flash column chromatography with gradually increasing 5–8% CH_2Cl_2 in hexanes to give product **6** (0.203 g, 73%) as an orange powder. FTIR (KBr) 2947, 2881, 2208, 1589, 1502, 1247, 1084, 1008, 840 cm^{-1}; ^1H NMR ($CS_2/CDCl_3$ (2:1), 500 MHz) δ 7.90 (d, J = 9.0 Hz, 2H), 7.81 (d, J = 9.0 Hz, 2H), 7.64 (d, J = 8.5 Hz, 2H), 7.61 (d, J = 8.5 Hz, 2H), 7.40 (d, J = 8.5 Hz, 2H), 7.20 (d, J = 8.5 Hz, 2H), 3.00–2.97 (m, 2H), 1.00–0.97 (m, 2H), 0.11 (s, 9H); ^{13}C NMR ($CS_2/CDCl_3$ (2:1), 125 MHz) δ 152.6, 152.0, 134.3, 132.5, 132.2, 131.3, 129.1, 128.5, 125.5, 124.2, 123.0, 91.1, 90.8, 30.3, 0.04; EI-HRMS m/z calcd for $C_{25}H_{25}BrN_2SSi$ 492.0691, found 492.0693.

(*E*)-1-(4-Bromophenyl)-2-(4-((trimethylsilyl)ethynyl)phenyl)diazene (8). See the general procedure for the Pd/Cu coupling reaction. The materials used were **7** (0.405 g, 1.05 mmol), TMSA (0.16 mL, 1.12 mmol), $PdCl_2(PPh_3)_2$ (0.016 g, 0.022 mmol), CuI (0.008 g, 0.040 mmol), TEA (5 mL), and THF (15 mL) at room temperature overnight. The residue was purified by flash column chromatography with 5% CH_2Cl_2 in hexanes to give product **8** (0.19 g, 51%) as an orange powder. FTIR (KBr) 3258, 2951, 2891, 2152, 1911, 1568, 1476, 1397, 1248, 1060, 846, 757, 558 cm^{-1}; ^1H NMR ($CS_2/CDCl_3$ (2:1), 500 MHz) δ 7.85 (d, J = 8.7 Hz, 2H), 7.81 (d, J = 8.8 Hz, 2H), 7.64 (d, J = 8.8 Hz, 2H), 7.55 (d, J = 8.7 Hz, 2H), 0.31 (s, 9H); ^{13}C NMR ($CS_2/CDCl_3$ (2:1), 125 MHz) δ 152.1, 151.9, 138.6, 133.1, 126.4, 124.7, 123.1, 104.8, 98.3, 97.6, 0.1; EI-HRMS m/z calcd for $C_{17}H_{17}BrN_2Si$ 356.0344, found 356.0340.

(*E*)-1-(4-(2-(12-Bromododecyloxy)ethyl)phenyl)-2-phenyldiazene (11). To a round-bottom flask equipped with a magnetic stirrer was added NaH (0.29 g, ~7.2 mmol, 60% dispersion in mineral oil) and DMF (14 mL). Compound **10** (0.46 g, 2.03 mmol) was added dropwise at room temperature. A deep red-brown mixture was formed, to which was added at once 1,12-dibromododecane (2.9 g, 8.84 mmol). The reaction mixture was stirred at room temperature for 20 h, then quenched with water and diluted with CH_2Cl_2. The aqueous layer was extracted with CH_2Cl_2 (×3). The combined organic layers were dried over $MgSO_4$, filtered, and concentrated under vacuum. Crude material was purified by flash column with gradually increasing 1–3% ethyl acetate in hexanes. The product was further purified using another flash column with the mixture of 1% ethyl acetate and gradually increasing 25–30% CH_2Cl_2 in hexanes to afford the product **11** (0.41 g, 43%) as an orange solid. FTIR (KBr) 3052, 2919, 2843, 2784, 1464, 1441, 1303, 1204, 1108, 845, 766, 684 cm^{-1}; ^1H NMR (400 MHz, $CDCl_3$) δ 7.91 (d, J = 8.5 Hz, 2H), 7.86 (d, J = 8.5 Hz, 2H), 7.53–7.47 (m, 3H), 7.39 (d, J = 8.5 Hz, 2H), 3.68 (t, J = 7.0 Hz, 2H), 3.45 (t, J = 6.7 Hz, 2H), 3.41 (t, J = 6.7 Hz, 2H), 2.97 (t, J = 7.0 Hz, 2H), 1.85 (quint, J = 7.0 Hz, 2H), 1.57 (m, 2H), 1.40 (m, 2H), 1.27 (m, 14H); ^{13}C NMR (100 MHz, $CDCl_3$) δ 153.0, 151.5, 143.0, 131.0, 129.8, 129.3, 123.1, 123.0, 71.6, 71.4, 36.5, 34.3, 33.1, 29.9, 29.80, 29.76, 29.74, 29.68, 29.65, 29.0, 28.4, 26.4; MALDI-TOF MS m/z (sulfur as the matrix) m/z calcd for $C_{26}H_{37}BrN_2O$ 472.2089, found 472.

(*E*)-1-(4-(2-(12-(4-Iodophenoxy)dodecyloxy)ethyl)phenyl)-2-phenyldiazene (12). To a round-bottom flask equipped with a magnetic stirrer were added **11** (0.41 g, 0.87 mmol), DMF (14 mL), 4-iodophenol (0.29 g, 1.29 mmol), and K_2CO_3 (0.5 g, 3.6 mmol). The reaction mixture was stirred at 90 °C for 12 h, and then NaI (0.1 g, 0.7 mmol), 4-iodophenol (0.5 g, 2.27 mmol), and K_2CO_3 (0.5 g, 3.6 mmol) were added. After stirring at 90 °C for 3 h, the reaction was quenched with water and diluted with CH_2Cl_2. The aqueous layer was extracted with CH_2Cl_2 (×3). Combined organic layers were dried over $MgSO_4$, filtered, and concentrated under vacuum. Crude material was purified by flash column with gradually increasing 1–30% CH_2Cl_2 in hexanes to afford the product **12** (0.28 g, 53%) as a yellow powder. FTIR (KBr) 2915, 2840, 1485, 1461, 1246, 1108 cm^{-1}; ^1H NMR (400 MHz, $CDCl_3$) δ 7.92 (d, J = 8.5 Hz, 2H), 7.86 (d, J = 8.5 Hz, 2H), 7.55–7.46 (m, 5H), 7.38 (d, J = 8.5 Hz, 2H), 6.67 (d, J = 8.5 Hz, 2H), 3.91 (t, J = 6.7 Hz, 2H), 3.68 (t, J = 7.0 Hz, 2H), 3.45 (t, J = 6.7 Hz, 2H), 2.97 (t, J = 7.0 Hz, 2H), 1.76 (quint, J = 7.0 Hz, 2H), 1.58 (m, 2H), 1.43 (m, 2H), 1.27 (m, 14H); ^{13}C NMR (100 MHz, $CDCl_3$) δ 159.2, 152.9, 151.4, 143.0, 138.4, 131.0, 129.8, 129.3, 123.1, 123.0, 117.2, 82.6, 71.6, 71.4, 68.3, 36.5, 29.9, 29.78, 29.76, 29.68, 29.57, 29.4, 26.4, 26.2; EI-HRMS m/z calcd for $C_{32}H_{41}IN_2O_2$ 612.2213, found 612.2229.

(*E*)-1-Phenyl-2-(4-(2-(12-(4-((trimethylsilyl)ethynyl)phenoxy) dodecyloxy)ethyl)phenyl)diazene (13). See the general procedure for the Pd/Cu coupling reaction. The materials used were **12** (0.28 g, 0.46 mmol), TMSA (1.0 mL, 7.0 mmol), $PdCl_2(PPh_3)_2$ (0.014 g, 0.020 mmol), CuI (0.008 g, 0.040 mmol), TEA (20 mL), and THF (10 mL) at room temperature overnight. The residue was purified by flash column chromatography with gradually increasing 1–33% CH_2Cl_2 in hexanes to give product **13** (0.22 g, 83%) as an orange powder. FTIR (KBr) 3068, 3036, 2909, 2841, 2155, 1599, 1051, 1465, 1242, 1104, 828 cm^{-1}; ^1H NMR (400 MHz, $CDCl_3$) δ 7.92 (d,J = 8.5 Hz, 2H), 7.86 (d, J = 8.5 Hz, 2H), 7.52–7.45 (m, 3H), 7.41–7.37 (m, 4H), 6.81 (d, J = 8.5 Hz, 2H), 3.94 (t, J = 6.7 Hz, 2H), 3.70 (t, J = 7.0 Hz, 2H), 3.45 (t, J = 6.7 Hz, 2H), 2.98 (t, J = 7.0 Hz, 2H), 1.77 (quint, J = 7.0 Hz, 2H), 1.58 (m, 2H), 1.43 (m, 2H), 1.27 (m, 14H), 0.25 (s, 9H); ^{13}C NMR (100 MHz, $CDCl_3$) δ 159.6, 152.9, 151.5, 143.0, 133.6, 131.0, 129.8, 129.3, 123.1, 123.0, 115.2, 114.5, 105.5, 92.5, 71.6, 71.4, 68.3, 36.5, 29.9, 29.79, 29.77, 29.68, 29.59, 29.39, 26.4, 26.2, 0.30; EI-HRMS m/z calcd for $C_{37}H_{50}N_2O_2Si$ 582.3642, found 582.3634.

Compound 16. See the general procedure for the Pd/Cu coupling reaction. The materials used were **15** (0.47 g, 0.78 mmol), **14** (0.15 g, 0.36 mmol), $PdCl_2(PPh_3)_2$ (0.010 g, 0.014 mmol), CuI (0.004 g, 0.021 mmol), TEA (20 mL), and THF (30 mL) at room temperature overnight. The residue was purified by flash column chromatography with gradually increasing 5–15% CH_2Cl_2 in hexanes to give the protected **16**. The orange oil was subsequently dissolved in THF (30 mL), TBAF (0.52 mL, 0.52 mmol) was added, and the mixture was stirred at room temperature for 1 h. The resulting solution was passed through a short silica plug and dried to give product **16** (0.21 g, 63% overall) as an orange oil. FTIR (KBr) 3283, 2919, 2843, 2208, 2094, 1589, 1513, 1459, 1410, 1214, 845 cm^{-1}; ^1H NMR (400 MHz, $CDCl_3$) δ 7.94 (d,J = 8.5 Hz, 4H), 7.69 (d, J = 8.5 Hz, 4H), 7.02 (s, 2H), 7.00 (s, 2H), 4.03 (m, 8H), 3.37 (s, 2H), 1.86 (m, 8H), 1.52 (m, 8H), 1.34 (m, 48H), 0.89 (m, 12H); ^{13}C NMR (100 MHz, $CDCl_3$) δ 154.6, 154.0, 152.2, 132.8, 126.8, 123.5, 118.2, 117.3, 114.6, 113.5, 95.1, 89.0, 82.9, 80.4, 79.4, 70.1, 70.06, 32.3, 32.0, 30.1, 29.99, 29,97, 29.85, 29.76, 29.7, 29.6, 26.5, 26.3, 23.1, 14.5; EI-MS m/z calcd for $C_{72}H_{98}N_2O_4$ 1054, found 1054.

(*E*)-1-Phenyl-2-(4-((trimethylsilyl)ethynyl)phenyl)diazene (23). See the general procedure for the Pd/Cu coupling reaction. The materials used were **22** (0.2 g, 0.65 mmol), TMSA (0.28 mL, 1.95 mmol), $PdCl_2(PPh_3)_2$ (0.005 g, 0.006 mmol), CuI (0.0025 g, 0.012 mmol), TEA (0.8 mL), and THF (9 mL) at room temperature for 20 min. The dark brown solid was purified by flash column chromatography with 5% CH_2Cl_2 in hexanes to give product **23** (0.12 g, 67%) as an orange powder. FTIR (KBr) 3057, 2962, 2898, 2154, 1594, 1492, 1250, 1223, 1152, 866, 843, 762, 588, 588 cm^{-1}; ^1H NMR (400 MHz) δ 7.91 (dd, J_1 = 8.0 Hz, J_2 = 1.6 Hz, 2H), 7.86 (d, J = 8.8 Hz, 2H), 7.60 (d, J = 8.8 Hz, 2H), 7.49 (m, 3H), 0.27 (s, 9H); ^{13}C NMR ($CDCl_3$, 100 MHz) δ 152.9, 152.2, 133.1, 131.6, 129.4, 126.1, 123.3, 123.1, 104.9, 97.3, 0.27; EI-HRMS m/z calcd for $C_{17}H_{18}N_2Si$ 278.1239, found 278.1244.

(*E*)-1-(4-Ethynylphenyl)-2-phenyldiazene (24). To a round-bottom flask equipped with a magnetic stirrer were added compound **23** (0.12 g, 0.43 mmol), THF (5 mL), and TBAF (0.8 mL, 0.8 mmol). The reaction mixture was stirred at room temperature for 20 min, then quenched with water and diluted with CH_2Cl_2. The aqueous layer was extracted with CH_2Cl_2 (×3). Combined organic layers were dried over $MgSO_4$, filtered, and concentrated under vacuum. Crude material was purified by flash column with 10% CH_2Cl_2 in hexanes to afford deprotected product **24** (0.086 g, 96%) as an orange-red solid. FTIR (KBr) 3290, 3260, 3196, 2924, 2564, 1515, 1493, 1483, 1265, 1154, 843 cm^{-1}; ^1H NMR ($CDCl_3$, 400 MHz) δ 7.93–7.87 (m, 4H), 7.63 (d, J = 8.4 Hz, 2H), 7.54–7.48(m, 3H), 3.22 (s, 1H); ^{13}C NMR ($CDCl_3$, 100 MHz) δ 152.6, 152.2, 133.0, 131.4, 129.2, 124.7, 123.0, 122.9, 83.3, 79.5; EI-HRMS m/z calcd for $C_{14}H_{10}N_2$ 206.0844, found 206.0842.

Acknowledgment. The Welch Foundation, DARPA/AFOSR, the NSF Penn State MRSEC and the NSF NIRT (Grant ECCS-0708765) program funded this work. The NSF, Grant CHEM 0075728, provided partial funding for the 400 MHz NMR. We thank Drs. I. Chester of FAR Research Inc. and R. Awartani of Petra Research Inc. for providing TMSA.

Supporting Information Available: Detailed NMR spectra for all new compounds and UV–vis spectra for selected compounds. This material is available free of charge *via* the Internet at http://pubs.acs.org.

REFERENCES AND NOTES

1. Tour, J. M. *Molecular Electronics: Commercial Insights, Chemistry, Devices, Architecture and Programming*; World Scientific: River Edge, NJ, 2003.
2. *Nanoelectronics and Information Technology: Advanced Electronic Materials and Novel Devices Information Technology*; Waser, R., Ed.; Wiley-VCH: Weinheim, Germany, 2003.
3. Timp, G. L. *Nanotechnology*; AIP Press/Springer: New York, 1999.
4. Joachim, C.; Gimzewski, J. K.; Aviram, A. Electronics Using Hybrid-Molecular and Mono-Molecular Devices. *Nature* **2000**, *408*, 541–548.
5. Forrest, S. R. The Path to Ubiquitous and Low-Cost Organic Electronic Appliances on Plastic. *Nature* **2004**, *428*, 911–918.
6. Shirai, Y.; Morin, J.-F.; Sasaki, T.; Guerrero, J. M.; Tour, J. M. Recent Progress on Nanovehicles. *Chem. Soc. Rev.* **2006**, *35*, 1043–1055.
7. Kay, E. R.; Leigh, D. A.; Zerbetto, F. Synthetic Molecular Motors and Mechanical Machines. *Angew. Chem., Int. Ed.* **2007**, *46*, 72–191.
8. Porto, M.; Urbakh, M.; Klafter, J. Atomic Scale Engines: Cars and Wheels. *Phys. Rev. Lett.* **2000**, *84*, 6058–6061.
9. Balzani, V.; Credi, A.; Venturi, M. *Molecular Devices and Machines - A Journey into the Nano World*; Wiley-VCH: Weinheim, Germany, 2004.
10. Feringa, B. E. *Molecular Switches*; Wiley-VCH: Weinheim, Germany, 2001.
11. Kelly, T. R., Ed. *Molecular Machines*; Topics in Current Chemistry 262; Springer: Heidelberg, Germany, 2005.
12. *Stimulating Concepts in Chemistry*; Shibaski, M., Stoddart J. F., Vogtle F., Eds.; Wiley-VCH: Weinheim, Germany, 2000.
13. Raymo, F. M.; Tomasulo, M. Electron and Energy Transfer Modulation with Photochromic Switches. *Chem. Soc. Rev.* **2005**, *34*, 327–336.
14. Browne, W. R.; O'Boyle, N. M.; McGarvey, J. J.; Vos, J. G. Elucidating Excited State Electronic Structure and Intercomponent Interactions in Multicomponent and Supramolecular Systems. *Chem. Soc. Rev.* **2005**, *34*, 641–663.
15. Morin, J.; Shirai, Y.; Tour, J. M. En Route to a Motorized Nanocar. *Org. Lett.* **2006**, *8*, 1713–1716.
16. Schuster, D. I.; Nuber, B.; Vail, S. A.; ManMahon, S.; Lin, C.; Wilson, S. R.; Khong, A. Synthesis, Photochemistry and Photophysics of Stilbene-Derivatized Fullerenes. *Photochem. Photobiol. Sci.* **2003**, *2*, 315–321.
17. Hartley, G. S. The cis-Form of Azobenzene. *Nature* **1937**, *140*, 281–282.
18. Shimoboji, T.; Larenas, E.; Fowler, T.; Kulkarni, S.; Hoffman, A. S.; Stayton, P. S. Photoresponsive Polymer-Enzyme Switches. *Proc. Natl. Acad. Sci. U.S.A.* **2002**, *99*, 16592–16596.
19. Yu, Y.; Nakano, M.; Ikeda, T. Directed Bending of a Polymer Film by Light. *Nature* **2003**, *425*, 145–156.
20. Yasuda, S.; Nakamura, T.; Matsumoto, M.; Shigekawa, H. Phase Switching of a Single Isomeric Molecule and Associated Characteristic Rectification. *J. Am. Chem. Soc.* **2003**, *125*, 16430–16433.
21. Ichimura, K.; Oh, S.-K.; Nakagawa, M. Light-Driven Motion of Liquids on a Photoresponsive Surface. *Science* **2000**, *288*, 1624–1626.
22. Kay, K.-Y.; Han, K.-J.; Yu, Y.-J.; Park, Y. D. Dendritic fullerenes (C_{60}) with Photoresponsive Azobenzene Groups. *Tetrahedron Lett.* **2002**, *43*, 5053–5056.
23. Prato, M. Fullerene Materials. *Top. Curr. Chem.* **1999**, *199*, 173–187.
24. Konishi, T.; Ikeda, A.; Shinkai, S. Supramolecular Design of Photocurrent-Generating Devices Using Fullerenes Aimed at Modelling Artificial Photosynthesis. *Tetrahedron* **2005**, *61*, 4881–4899.
25. Segura, J. L.; Martín, N.; Guldi, D. M. Materials for Organic Solar Cells: The C_{60}/π-Conjugated Oligomer Approach. *Chem. Soc. Rev.* **2005**, *34*, 31–47.
26. Bunz, U. H. F. Poly(aryleneethynylene)s: Syntheses, Properties, Structures, and Applications. *Chem. Rev.* **2000**, *100*, 1605–1644.
27. Schwab, P. F. H.; Levin, M. D.; Michl, J. Molecular Rods. 1. Simple Axial Rods. *Chem. Rev.* **1999**, *99*, 1863–1933.
28. Shirai, Y.; Osgood, A. J.; Zhao, Y.; Kelly, K. F.; Tour, J. M. Directional Control in Thermally Driven Single-Molecule Nanocars. *Nano Lett.* **2005**, *5*, 2330–2334.
29. Shirai, Y.; Osgood, A. J.; Zhao, Y.; Yao, Y.; Saudan, L.; Yang, H.; Yu-Hung, C.; Sasaki, T.; Morin, J.-F.; et al. Surface-Rolling Molecules. *J. Am. Chem. Soc.* **2006**, *128*, 4854–4864.
30. Tour, J. M.; Rawlett, A. M.; Kozaki, M.; Yao, Y.; Jagessar, R. C.; Dirk, S. M.; Price, D. W.; Reed, M. A.; Zhou, C.-W.; Chen, J.; et al. Synthesis and Preliminary Testing of Molecular Wires and Devices. *Chem.—Eur. J.* **2001**, *7*, 5118–5134.
31. Liao, L.-X.; Stellacci, F.; McGrath, D. V. Photoswitchable Flexible and Shape-Persistent Dendrimers: Comparison of the Interplay between a Photochromic Azobenzene Core and Dendrimer Structure. *J. Am. Chem. Soc.* **2004**, *126*, 2181–2185.
32. Flatt, A. K.; Dirk, S. M.; Henderson, J. C.; Shen, D. E.; Su, J.; Reed, M. A.; Tour, J. M. Synthesis and Testing of New End-Functionalized Oligomers for Molecular Electronics. *Tetrahedron* **2003**, *59*, 8555–8570.
33. Yu, B.-C.; Shirai, Y.; Tour, J. M. Syntheses of New Functionalized Azobenzenes for Potential Molecular Electronic Devices. *Tetrahedron* **2006**, *62*, 10303–10310.
34. Shirai, Y.; Zhao, Y.; Cheng, L.; Tour, J. M. Facile Synthesis of Multifullerene-OPE Hybrids via in Situ Ethynylation. *Org. Lett.* **2004**, *6*, 2129–2132.
35. Ueno, A.; Takahashi, K.; Anzai, J.-I.; Osa, T. Solvent-Induced Conformational Changes of Arylazo-Substituted Polyaspartates. *Bull. Chem. Soc. Jpn.* **1980**, *53*, 1988–1992.
36. Zhao, Y.; Shirai, Y.; Slepkov, A. D.; Cheng, L.; Alemany, L. B.; Sasaki, T.; Hegmann, F. A.; Tour, J. M. Synthesis, Spectroscopic and Nonlinear Optical Properties of Multiple [60]Fullerene-Oligo(*p*-phenylene ethynylene) Hybrids. *Chem.—Eur. J.* **2005**, *11*, 3643–3658.
37. Meier, H.; Ickenroth, D.; Stalmach, U.; Koynov, K.; Bahtiar, A.; Bubeck, C. Preparation and Nonlinear Optics of Monodisperse Oligo(1,4-phenyleneethynylene)s. *Eur. J. Org. Chem.* **2001**, 4431–4444.
38. Nishikawa, T.; Shibuya, S.; Hosokawa, S.; Isobe, M. One Pot Synthesis of Haloacetylenes from Trimethylsilylacetylenes. *Synlett* **1994**, 485–486.
39. Kim, S.; Kim, S.; Lee, T.; Ko, H.; Kim, D. A New, Iterative Strategy for the Synthesis of Unsymmetrical Polyynes: Application to the Total Synthesis of 15,16-Dihydrominquartynoic Acid. *Org. Lett.* **2004**, *6*, 3601–3604.
40. Grebel-Koehler, D.; Liu, D. J.; De Feyter, S.; Enkelmann, V.; Weil, T.; Engels, C.; Samyn, C.; Mü llen, K.; De Schryver, F. C. Synthesis and Photomodulation of Rigid Polyphenylene Dendrimers with an Azobenzene Core. *Macromolecules* **2003**, *36*, 578–590.
41. Schulte-Frohlinde, D. Über den Mechanismus der Katalytischen *cis-trans* Umlagerung von Azobenzol. *Justus Liebigs Ann. Chem.* **1958**, *612*, 131–138.
42. *Fullerenes: From Synthesis to Optoelectronic Properties*; Guldi, D. M., Martin, N., Eds.; Kluwer Academic Publishers: Dordrecht, The Netherlands, 2002.
43. Guldi, D. M.; Prato, M. Excited-State Properties of C_{60} Fullerene Derivatives. *Acc. Chem. Res.* **2000**, *33*, 695–703.

44. Åstrand, P. -O.; Ramanujam, P. S.; Hvilsted, S.; Bak, K. L.; Sauer, S. P. A. Ab Initio Calculation of the Electronic Spectrum of Azobenzene Dyes and Its Impact on the Design of Optical Data Storage Materials. *J. Am. Chem. Soc.* **2000**, *122*, 3482–3487, and references therein.
45. Fischer, E. Photosensitized Isomerization of Azobenzene. *J. Am. Chem. Soc.* **1968**, *90*, 796–797.
46. Yamamura, T.; Momotake, A.; Arai, T. Synthesis and Photochemical Properties of Porphyrin-Azobenzene Triad. *Tetrahedron. Lett.* **2004**, *45*, 9219–9223.
47. Jones, L. B.; Hammond, G. S. Mechanisms of Photochemical Reactions in Solution. XXX. Photosensitized Isomerization of Azobenzene. *J. Am. Chem. Soc.* **1965**, *87*, 4219–4220.
48. Bortolus, P.; Monti, S. Cis-Trans Photoisomerization of Azobenzene. Solvent and Triplet Donor Effects. *J. Phys. Chem.* **1979**, *83*, 648–652.
49. Hamasaki, R.; Ito, M.; Lamrani, M.; Mitsuishi, M.; Miyashita, T.; Yamamoto, Y. Nonlinear Optical Studies of Fullerene-Arylethyne Hybrids. *J. Mater. Chem* **2003**, *13*, 21–26, and references therein.
50. Change in absorption (Δabs) for the main absorption band of the *trans* isomer (π,π^*) transition band ($\lambda_{max} \approx$ 330–400 nm) reflects the minimum concentration of *cis* isomer at the photostationary state; see refs 51 and 52.
51. King, N. R.; Whale, E. A.; Davis, F. J.; Gilbert, A.; Mitchell, G. R. Effect of Media Polarity on the Photoisomerisation of Substituted Stilbene, Azobenzene and Imine Chromophores. *J. Mater. Chem.* **1997**, *7*, 625–630.
52. Brode, W. R.; Gould, J. H.; Wyman, G. M. The Relation between the Absorption Spectra and the Chemical Constitution of Dyes. XXV. Phototropism and cis-trans Isomerism in Aromatic Azo Compounds. *J. Am. Chem. Soc.* **1952**, *74*, 4641–4646.
53. Yu, C. J.; Chong, Y.; Kayyem, J. F.; Gozin, M. Soluble Ferrocene Conjugates for Incorporation into Self-Assembled Monolayers. *J. Org. Chem.* **1999**, *64*, 2070–2079.
54. Morin, J.-F.; Sasaki, T.; Shirai, Y.; Guerrero, J. M.; Tour, J. M. Synthetic Routes toward Carborane-Wheeled Nanocars. *J. Org. Chem.* **2007**, *72*, 9481–9490.